Conjugation length dependence of Raman scattering in a series of linear polyenes: Implications for polyacetylene

H. E. Schaffer, R. R. Chance, R. J. Silbey, K. Knoll, and R. R. Schrock

Additional information on J. Chem. Phys.

Conjugation length dependence of Raman scattering in a series of linear polyenes: Implications for polyacetylene

H. E. Schaffer
Exxon Research and Engineering Company, Corporate Research Laboratories, Annandale, New Jersey 08801

R. R. Chance
Exxon Chemical Company, PARAMINS Technology Division, Linden, New Jersey 07036

R. J. Silbey, K. Knoll,[a] and R. R. Schrock
Massachusetts Institute of Technology, Department of Chemistry and Center for Materials Science and Engineering, Cambridge, Massachusetts 02139

We have measured the solid state Raman scattering spectra of a homologous series of linear polyenes, with the number of alternated double bonds varying from 3 to 12. While we find a linear dependence of the Raman shifts of resonantly coupled modes with inverse conjugation length, we have also followed the suggestion of previous work in examining the inverse square product of the several Raman frequencies as a function of the logarithm of the measured energy gap of the molecule. This provides a linear relationship, as found for *trans*-polyacetylene, a result which is qualitatively consistent with the amplitude mode model of Horovitz and co-workers. We also find, consistent with previous work on polyacetylene, a monotonic decrease in the ratios of oscillator strengths of the two strongest bands with conjugation length, as recently predicted by a series of molecular dynamics calculations. Suggested interpretations of a number of qualitative observations, including splitting of modes for shorter conjugation length, are offered, and the implications for the structure of *trans*-polyacetylene are discussed. The present work confirms that the previously measured dispersion in the Raman spectra of *trans*-polyacetylene is due to a distribution of conjugation lengths and brings into question some of the quantitative aspects of the amplitude mode model.

I. INTRODUCTION

A controversial issue in the spectroscopy of *trans*-polyacetylene has been the dispersive behavior of the measured Raman scattering spectra.[1-6] For red laser excitation, two strongly resonantly enhanced peaks are seen; the first, at ~ 1060 cm^{-1}, is in the region usually characteristic of carbon–carbon single bond stretch modes, while the second, at ~ 1460 cm^{-1}, is similarly associated with a carbon–carbon double bond stretch. Both observed modes have asymmetric band shapes. As the excitation wavelength is decreased toward the blue, both of these bands develop pronounced shoulders on the high frequency side. The frequencies of the shoulders increase monotonically with increasing laser photon energy until they are resolved as satellites for blue excitation. While the positions of the primary peaks (those observed for red excitation) remain unchanged with excitation wavelength, the dispersive behavior of the satellites shows a sample dependence.

There have been two main schools of interpretation of these data. The first,[7,8] due to Brivio and Mulazzi, among others, is based upon the observation of linear decrease of Raman shift with the inverse of the conjugation length (number of conjugated double bonds) in various sets of conjugated polyenes.[9,10] A distribution of conjugation lengths within a given sample of polyacetylene is assumed. For a given conjugation length, the expression for the Raman cross section, as calculated from standard second-order perturbation theory via consideration of excited states,[11] is somewhat complicated, but the dependence of the spectrum on the Raman shift is simply that of a narrow Gaussian band centered at the frequency obtained by extrapolation of the linear polyene data to the given conjugation. This model, when applied to the experimental data described above, provides a direct measure of the distribution of conjugation lengths within a given sample. In particular, the dispersive data described above is correlated with a *bimodal* distribution of conjugation lengths,[8,12] so that the sample dependence of the Raman spectra is then due to a varied distribution of conjugation lengths. The bimodal result has been criticized as "unphysical." However, there is no physical argument to preclude such a result and at least one physical reason to expect it—namely, the well-known fact that polyacetylene contains crystalline and amorphous regions.

The conjugation length is not an explicit parameter in the second of the two approaches, known as the "amplitude mode" (AM) model, nor are the excited states directly considered.[6,13-16] The AM description involves a charge density wave ground state of period a, where a is the polyene chain unit cell length, a dimensionless electron–phonon coupling constant λ, and a related "phonon renormalization parameter" $\bar{\lambda}$ (see below). The resulting cross section has a simpler form than that of the first model; it is the product of two functions. The first contains the resonance effect, peaking

---

when the laser photon energy equals E_g; the second explicitly depends upon $\tilde{\lambda}$, having peaks that increase in frequency for increasing $\tilde{\lambda}$. This form allows a unimodal distribution in $\tilde{\lambda}$ to explain the observed bimodal spectra[16]; each observed peak corresponds to the peak of one of the two product functions. In particular, the primary peak corresponds to the most probable value of $\tilde{\lambda}$ (peak of second component function), while the satellite corresponds to the value of $\tilde{\lambda}$ associated with the pump photon energy (peak of first component function). It should be noted that this model also provides an explanation for infrared absorptions generated by reduction or oxidation of polyacetylene, as well as by photogeneration of charged defects.[16] The dispute between this model and the previous one has been presented in the literature.[15,17]

For the purposes of the present work, two aspects of the second model are critical. The first is the assumption of the existence of a set of (three) coupled (to the π electron energy) normal modes of the polyene chain, whose eigenvectors and bare frequencies are independent of $\tilde{\lambda}$.[13] By bare frequency is meant the (fictional) frequency of the mode for the σ core alone, i.e., in the absence of coupling to the π electrons. The parameter $\tilde{\lambda}$ renormalizes the phonon frequencies, giving rise to a decrease in Raman frequencies with decreasing $\tilde{\lambda}$. The second is the conclusion of Ehrenfreund *et al.*, within the context of their model, that the derived distribution in $\tilde{\lambda}$ does not correspond to a distribution in conjugation lengths, but rather to another (unnamed) type of disorder that provides a distribution in λ and $\tilde{\lambda}$.[16]

In this paper we present the Raman spectra of a comprehensive series of unsubstituted *t*-butyl end-capped all-*trans* polyenes, with the number of double bonds N varied between 3 and 12.[18] While we do find, in accord with previous workers,[9,10] a linear decrease in the Raman frequencies of the two most strongly resonantly enhanced bands with inverse conjugation (for $N \geqslant 7$), we have also analyzed the measured Raman shifts in the framework of the AM model. This analysis allows us to probe the validity of the assumption of bare phonon frequencies independent of $\tilde{\lambda}$, as well as the assertion that the disorder in *trans*-polyacetylene is not primarily due to a distribution of conjugation lengths. We have also attempted to analyze the combined frequency and intensity data by consideration of the predicted integrated cross sections, to test the model further. Our discussion of the AM model is influenced by the more recent work[19-24] on polyene vibrational frequencies of Zerbi and co-workers which, while attempting to explain the results of the AM model in terms of molecular dynamics, simultaneously contests the critical assumption mentioned above. The remainder of the paper is organized as follows: Section II provides an exposition of the details of the data collection, and Sec. III presents the spectra and catalogs the measured frequencies and integrated oscillator strengths. The data are discussed in terms of the AM model in Sec. IV, and a conclusion is finally provided.

II. EXPERIMENTAL METHODS

The synthesis and characterization of the polyene samples used in these experiments have been described in detail

elsewhere.[18] Though polyenes with well-defined *cis* structures were prepared and studied, this report will consider only the all-*trans* isomers. After preparation, the samples, in the form of powder or small crystallites, were stored at low temperature, in the dark, and under argon in glass vials. The integrities of the vial seals were judged by noting the absence of any ice on the inside of the cooled vials, as well as the reproducibility of Raman spectra taken before and after several months of storage. By contrast, samples exposed to ambient atmosphere visibly decomposed to an off-white color in a matter of hours. The 0-ene, hexamethyl-ethane, was purchased 99% pure from Aldrich Chemical and used without further purification.

For the Raman scattering measurements, the vials were allowed to warm to room temperature and then placed directly into the spectrometer such that the sample within the vial was at the focal point of the collecting optics, which were set in near-backscattering geometry. The spectra were measured at ambient temperature thus preventing collection of high quality data for the volatile 1-ene and 2-ene. Excitation was provided by one of the 6764, 6471, or 5309 Å lines from a Kr$^+$ laser, or the 5017 Å line from a Ar$^+$ laser. The excitation wavelength was chosen to be below our measured solid state absorption energy thus eliminating the need for drastic correction for reabsorption of emitted light and avoiding photochemical modification and broadband fluorescence. All data collections were bracketed by a preliminary and final measurement of the scattering intensity at one of the strong peaks, to ensure that sample degradation had not altered the spectra. Incident powers were typically 3 to 10 mW.

Raman scattering data were recorded with either of two instruments. The first was a Spex Triplemate spectrometer terminated with a EG&G Princeton Applied Research model 1420 silicon photodiode array detector. The diode array provided a range of approximately 350 cm^{-1}, with a spacing of about 0.7 cm^{-1} between array elements, centered at the set wavelength of the Triplemate; the range was calibrated for wave number Raman shift from a particular exciting laser wavelength using known emission lines from low pressure inert gas bulbs. The data collection was managed by a PAR model 1460 optical multichannel analyzer. A preliminary report of these results appeared recently.[25] The second instrument was a Spex scanning triple monochromator, equipped with a spatial filter between the first and second stages to further enhance stray light rejection, terminated with a cooled RCA C31034-A02 photomultiplier tube operating in photon counting mode. In this latter case, the collection of data, the 2 cm^{-1} intervals, was managed by a Spex Datamate computer. The entrance slit was set at 1 mm, providing a bandpass of approximately 10 cm^{-1} for previously reported data.

The diode array instrument has demonstrated irreproducibility of as much as 5 cm^{-1} as determined by the variation in known rare gas lines when the grating position is moved away and then returned. Therefore, except where noted, the data reported here were collected with the scanning instrument, which has been calibrated with the 6328 Å line of helium–neon laser, with 1.0 cm^{-1} intervals and 1.9

cm^{-1} spectral bandpass at 1300 cm^{-1} shift. The data reported here are roughly 2 cm^{-1} higher than our previous set.[25] We have confidence that the accuracy of the Raman shifts reported is $\pm 1 cm^{-1}$. The sample of the longest molecule, the 13-ene, was unfortunately unavailable for experiments on the scanning instrument, so that we are unable to report a more accurate value for its shifts. All spectra presented here were corrected for the spectral response of the collecting optics/monochromator/photomultiplier tube by calibration with a blackbody spectral standard manufactured by Gamma Scientific.

The spectra were transferred to a PC for analysis. Peak positions were determined with a center of mass algorithm[26] with the half-maximum intensity used as the cutoff coded for SPECTRACALC software (Galactic Industries, Salem, NH). In the calculation of center of mass peak positions, integrated oscillator strengths, and full widths at half-maximum, routines written by us for use with SPECTRACALC allowed interactive subtraction of best fit by eye polynomial or Lorentzian backgrounds from peaks (e.g., peak R 1 from R 2, see below for labeling of peaks, or spectral background from all peaks) and replacement of overlaid peaks (e.g., R 2 over R 1) with best fit polynomial/Lorentzian interpolations.

III. RESULTS

Raman spectra were collected between 10 and 1900 cm^{-1} for the 0-ene and the 3–12-enes. The spectrum of one of the molecules, the 7-ene, is shown in Fig. 1, in which the upper curve is an expansion of the lower curve by a factor of 20. The salient observation is that the strongest peaks are found in the region 800–1800 cm^{-1}, in this and all other members of the series. The resonant enhancement of th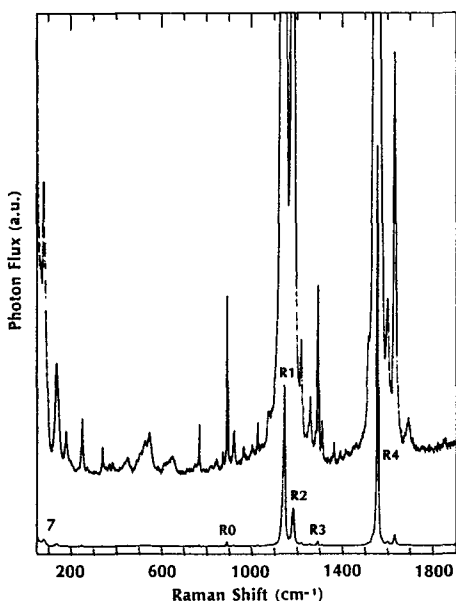e peaks in this range is due to coupling to the dimerization amplitude, i.e., the intensities are primarily due to π-electron polarizability and the coupling of these vibrational modes to the lowest energy excited state. We thus restrict our discussion in this paper to this region. The multitude of weaker peaks, particularly below 1100 cm^{-1}, are presumably due to normal modes that have large components out of the plane of conjugation, and are thus coupled only weakly to the excited state. These modes have oscillator strength largely due to σ electron polarizability, which is not considered in the model of Horovitz *et al.*[6,13-16] to be discussed below.

The Raman spectra in the range 1000–1800 cm^{-1} for the N-enes, $N = 0,3$–12, are presented in Fig. 2. The spectrum of the 0-ene is consistent with previous work.[27] The vertical scales have all been normalized such that the strongest peaks of the polyene spectra have the same height. The two strongest peaks, which are seen in the 12-ene spectrum at 1122 and 1506 cm^{-1}, and which are henceforth referred to as R 1 and R 4, respectively, correspond to the two most strongly resonantly enhanced peaks in polyacetylene, seen at 1065 and 1460 cm^{-1} for red excitation.[1-6] For all of the polyenes considered here, the Raman shifts are independent of excitation frequency, confirming the equivalence of chain length and conjugation length.

Several trends are immediately apparent from Fig. 2. The first is the behavior of the shifts as a function of conjugation length. While R 4 is seen to decrease monotonically with increasing conjugation, R 1 first increases between $N = 3$ and $N = 5$ and then decreases. This may be understood qualitatively by invoking coupling to the R 2 mode, which is seen in the 4-ene, e.g., at 1198 cm^{-1}, and which corresponds to the carbon–carbon single bond stretch band at 1238 cm^{-1} in the 0-ene. As the conjugation length decreases, the *t*-butyl end groups become relatively more significant, and the R 1 band, which would otherwise continue to increase is repelled downward by mixing with the R 2 mode. It should be noted

FIG. 1. Raman scattering spectrum of (*t*-butyl)–(HC = CH)$_7$–(*t*-butyl), or 7-ene, collected at ambient temperature and corrected for response of collecting optics/monochromator/detector. Upper curve is an expansion of lower curve by a factor of 20.
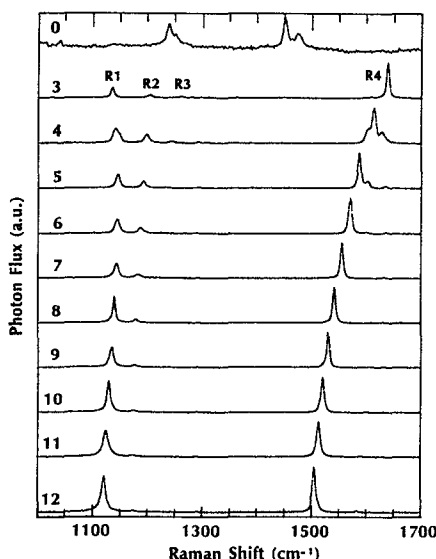

FIG. 2. Raman scattering spectra of *t*-butyl capped polyenes, for 3 to 12 double bonds, as well as the 0-ene, di(*t*-butyl). Spectra were collected at ambient temperature and were corrected for response of collecting optics/monochromator/detector.

that the 1173 cm^{-1} position of the R 2 frequency for the 12-ene is close to the 1176 cm^{-1} position of one band reported to be present in polyacetylene for excitation at 4579 Å but not for longer wavelength and for which no interpretation has been offered.[5] There is an apparent splitting of the R 4 mode in the 4-ene and 5-ene, for which we do not have an explanation at the present time.

In Fig. 3 we have plotted the frequencies of the R 1 and R 2 modes as a function of inverse conjugation or chain length, as has been previously suggested by several groups and as is commonly done for optical absorption frequencies. For comparison, we have also plotted our previously published data for the R 1 shifts. The best fit line (not shown) through the R 1 shifts for n = 8 through 12 has the form

$$\omega_{R1} = (A_1 + B_1/N) \text{ cm}^{-1}, \quad (1)$$

with $A_1 = 1082$ and $B_1 = 476$. These are different from the values used by other workers[8] in their analysis of the Raman scattering of polyacetylene, $A_1 = 1060$ and $B_1 = 600$.[8] However, the validity of this linear extrapolation, especially in light of the value of the R 1 shift for the 13-ene, as well as certain theoretical results, will be considered in more detail below. We have also plotted (Fig. 4) the variation of the R 4 shift against inverse conjugation, again plotting a best fit line through the data for N = 7 through 12. Using a form similar to that of Eq. (1), we find $A_4 = 1438$ and $B_4 = 830$. These values are close to those we have previously reported[25] for the range N = 7 through 12, $A_4 = 1430$ and $B_4 = 840$, and again vary somewhat from those used by other authors, $A = 1450$, $B = 500$.[8] In polyacetylene, a fourth band, at ~1291 cm^{-1}, has been seen slightly changed with respect to excitation wavelength,[6] and in these polyenes we have found a slight measurable shift of this band, which we call R 3, with chain length: It moves from 1291.3 cm^{-1} in the 12-ene to

FIG. 4. Raman shifts in carbon–carbon double bond region as a function of inverse conjugation. The circles represent present data, and the triangles are data previously reported for the same molecules. The line is a least squares fit for the data for N = 7–12.

1293.3 PW$_{-1}$ in the 7-ene.

As we have previously shown[25] the absorption maximum for the lowest energy optical transition in these polyenes also has a linear dependence upon inverse conjugation [in the solid state, E_g (cm^{-1}) = (11 000 + 79 000/N) for $N \geqslant 7$], as in the case in general for polyenes.[28-31] Therefore, at least over the conjugation range considered here, the nominal "carbon–carbon double bond stretch," or R 4, has a linear dependence upon the band gap, which is a simpler relationship than one proposed based upon a vibronic coupling model.[32] The variations of the R 1 and R 4 shifts as a function of absorption maximum are plotted in Fig. 5. For comparison, we have plotted previously published data[6,16] showing the dependence of the Raman satellite shifts in polyacetylene
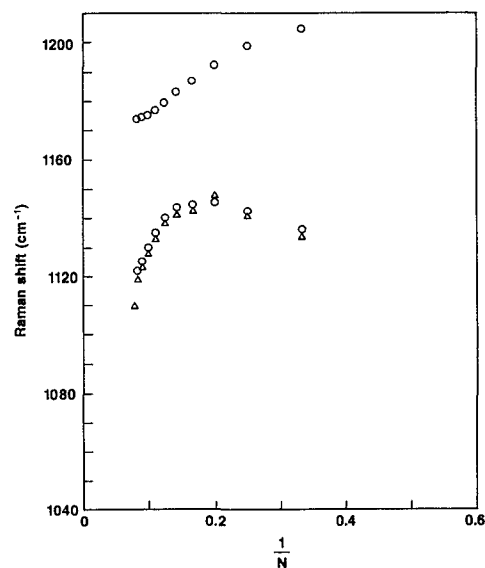

FIG. 3. Raman shifts in carbon–carbon single bond stretch region as a function of inverse conjugation. N is number of double bonds in molecule. The circles represent present data obtained with the scanning instrument, and the triangles are data previously reported for same molecules and obtained with diode array instrumentation (Ref. 25).
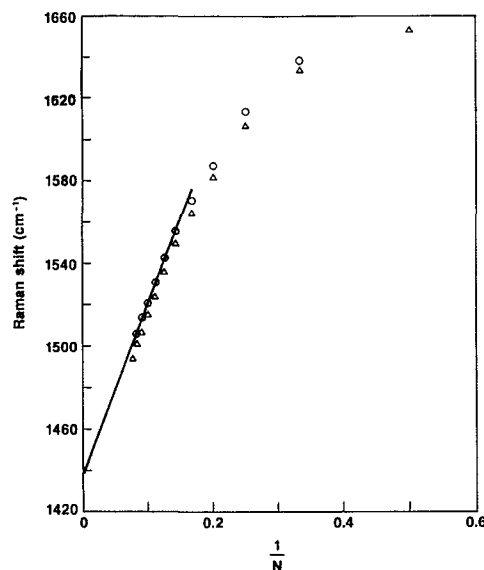
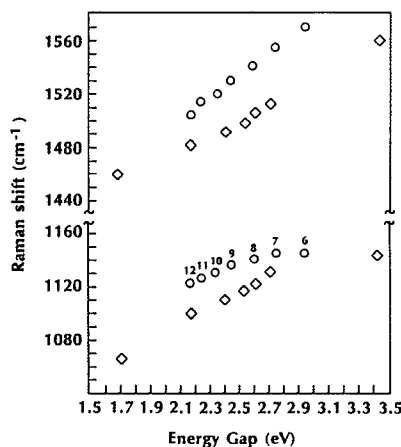

FIG. 5. Comparison of Raman shift as a function of photon energy for t-butyl capped polyenes vs polyacetylene. For the polyenes (circles), the abscissa is the measured solid-state energy, (Ref. 25) while for the polyacetylene (triangles), the abscissa is the photon excitation energy. The data for polyacetylene are taken from Ref. 16.

upon excitation photon frequency. In this amplitude mode model this corresponds to a resonance condition $\hbar\omega_L = E_g(\tilde{\lambda})$. The depressions of the shifts for polyacetylene with respect to those of these polyenes vary from between 10 and 25 cm^{-1} for R 1 and 25 to 40 cm^{-1} for R 4. Possible reasons for this divergence will be discussed below. Similar results are obtained when comparing Raman spectra of oligomers of polydiacetylene to photoselection results for conformationally disordered polydiacetylenes in solution.[33,34]

Since the spectra of Fig. 2 are all normalized such that R 4 peak has the same height, it can be seen that the ratio of the integrated intensities of the strongest bands, I_{R1}/I_{R4}, increases with increasing conjugation. It can also be seen that the ratio I_{R2}/I_{R1} decreases with increasing chain length, as would be expected as the t-butyl end groups compose a smaller fraction of the molecule. In Fig. 6 we have plotted the ratios (I_{R1}/I_{R4}), (I_{R2}/I_{R4}), and $[(I_{R1} + I_{R2})/I_{R4}]$ as a function of inverse conjugation length; the relative oscillator strengths, along with the frequencies for the R modes and the solid-state $(1B_u \leftarrow 1A_g)$ 0–0 absorption peaks,[25] are tabulated in Table I. The increase in the second of these three ratios is trivially due to the greater weight of the capping groups as the molecule becomes shorter, so that it is the decrease that is the physically significant result. Recalling that decreased conjugation length corresponds to higher band gap, we note that this trend is in qualitative agreement with the increase in the inverse ratio (I_{R4}/I_{R1}) with increasing excitation energy reported for polyacetylene.[16] In the case of the polymer, this variation has been shown to be consistent with the amplitude mode model, and recently the group of Zerbi and co-workers has proposed a reformulation of this in terms of molecular vibrational dynamics that would microscopically account for this trend in polyene series.[19–23]

In Fig. 7, we have amplified the vertical scale of Fig. 2 by a factor of 30, and have extended the wave number domain to show the modes at around 900 cm^{-1}. It is clear that as the chain length decreases, the spectra become significantly

more complicated. For example, R 3 is a single peak for the 12-ene but is split into three peaks for the 3-ene. This splitting is due interaction of the C–H bending mode for the polyene moiety with those of the methyl groups of the caps; this effect has been demonstrated in the comparison of the spectra of E-1,3,5-hexatriene (singlet) vs E,E,E-2,4,6-octatriene (triplet).[35] Furthermore, there is obviously a peak, seen to the immediate left of this triplet in the 3-ene (at 1262 cm^{-1}), that decreases in intensity and frequency with increasing conjugation. We suggest assignment of this peak to splitting of the R 2 peak due to interaction of the two single bonds connecting the capping t-butyl groups to the terminal double bonds; as the chain length increases, the interaction between the two ends decreases until they no longer interact, leading to a single frequency for the longer polyenes. This assignment is consistent with the observation of only one band in the carbon–carbon single bond stretch region at 1192 cm^{-1} in uncapped hexatriene.[36] A number of further noteworthy qualitative observations may be made. (1) There are two modes in the 0-ene, at 877 and 922 cm^{-1}, that propagate into the polyenes. The upper one shows negligible frequency shift as its intensity decreases with chain length. The lower of the two, however, varies monotonically from 889 cm^{-1} in the 6-ene to 897 cm^{-1} in the 12-ene; the curious fact that its frequency increases with increasing conjugation is explained below. (2) A band is seen at 1025 cm^{-1}, which may correspond to a similarly placed band seen in polyacetylene for excitation at 4765 Å, but not at 6459 Å.[16] As with the band at 1176 cm^{-1} noted above, this suggests that the polymer segments, having shorter conjugation which are photoselected at shorter laser wavelengths, show significant chain-end effects in the vibrational spectrum. And (3) there is a doublet on the blueshifted side of R 4, in which the relative oscillator strength of the lower (higher) shifted peak increases (decreases) with increasing conjugation. While, by frequency, these modes involve double bond stretching, they evidently have minimal resonant enhancement. Zerbi and co-workers have suggested[20] that such peaks may be due to scattering from $k \neq 0$ phonons (Horovitz only considered $k = 0$)[13] and furthermore that they are correlated with low intensity peaks seen in the photoinduced infrared absorption spectrum of *trans*-polyacetylene.[37,38] Confirmation of this assignment would be provided by calculation of matrix elements for scattering from the $k > 0$ phonons that reproduces the conjugation length dependence of the oscillator strength ratio. If this is indeed the case, then we have here provided, by Raman scattering rather than neutron scattering, the first fragmentary data on the phonon dispersion of this mode in polyenes. An alternative explanation would probably involve splitting of the R 4 mode due to nonuniform dimerization amplitude through the chain. Such an interpretation along with a more analytic discussion of these results in light of the work of the Milan group, will be discussed in future work.
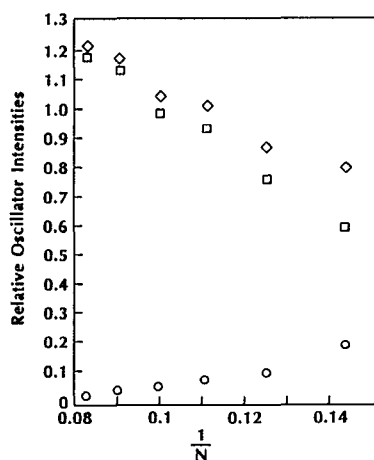

FIG. 6. Ratios of integrated oscillator strengths as a function of inverse conjugation. The squares are the R 1 intensities, the circles are R 2 intensities, and the diamonds are the sum of the previous two. In all cases, the oscillator strengths are with respect to that of R 4.

IV. DISCUSSION

In this section, we discuss the relevance of the new data on the short chain polyenes for the interpretation of the spec-

TABLE I. uv–visible absorption peaks (Ref. 25), Raman frequencies, and relative oscillator strengths ratios of resonantly coupled modes of *t*-butyl capped polyenes. N is number of double bonds. Units for uv–vis data are eV: units for Raman data ($R\,0 \rightarrow R\,4$) are cm^{-1}.

N	uv–vis Solid	uv–vis Pentane	R 0	R 1	R 2	R 3	R 4	I_{R0}/I_{R1}	I_{R1}/I_{R4}	I_{R2}/I_{R4}	I_{R3}/I_{R4}
0	⋯	⋯	877.4	⋯	1238.0	⋯	⋯	⋯	⋯	⋯	⋯
3	⋯	4.50	880.2	1136.1	1204.7	⋯	1638.5	⋯	⋯	⋯	⋯
4	⋯	3.98	885.6	1142.5	1198.7	⋯	1613.8	⋯	⋯	⋯	⋯
5	⋯	3.62	887.5	1145.4	1192.3	1292.7	1587.3	⋯	⋯	⋯	⋯
6	2.94	3.34	889.5	1144.5	1186.9	1290.2	1570.6	0.0043	0.56	0.19	0.017
7	2.75	3.13	891.9	1143.7	1183.2	1293.3	1555.6	0.0073	0.61	0.21	0.015
8	2.60	2.96	893.3	1140.1	1179.4	1292.4	1542.2	0.0064	0.76	0.11	0.015
9	2.45	2.83	894.7	1134.9	1176.8	1291.7	1530.9	0.0051	0.93	0.08	0.011
10	2.35	2.72	895.5	1129.8	1175.2	1291.0	1520.9	0.0081	0.98	0.06	0.012
11	2.25	2.64	896.1	1125.1	1174.6	1291.9	1514.0	0.0081	1.13	0.04	0.010
12	2.18	⋯	897.1	1121.8	1173.9	1291.3	1505.9	0.0110	1.18	0.03	0.011

tra of polyacetylene. In particular, we discuss the questions of conjugation lengths, chain end effects, oscillator strengths, and the interpretation of the disorder parameter $\bar{\lambda}$ introduced by Horovitz *et al.*[6,13–16]

In Fig. 2, we have shown that the frequencies of the Raman lines labeled $R\,1$ and $R\,4$ (the nominal single and double bond stretches) vary linearly with $1/N$ for $N = 7$ through 12. Since the polyenes we have examined are fully conjugated, i.e., the conjugation length is equal to the length of the molecule, we can ask what the present data suggest for the conjugation length of polyacetylene. Since polyacetylene films have a Raman line at 1460 cm^{-1}, a naive extrapolation of our data suggests that polyacetylene films have a conjugation length of $\sim$40 double bonds. A similar extrapolation of our $R\,1$ data (for $N = 7$ to 12) yields an infinite conjugation length for polyacetylene, since the polyacetylene frequency is 1065 cm^{-1}, *below* our extrapolated value. However, our initially measured value for $R\,1$ for the 13-ene (1110 cm^{-1}),

if included in our data set, would substantially lower the value of A_1 in Eq. (2), and hence would also yield a finite conjugation length for polyacetylene for $\sim$30–40 double bonds. As noted earlier our 13-ene sample had been destroyed by the time we switched to the more accurate scanning monochromator and we do not have a more accurate number for the Raman shift of this compound. Thus we can say that our data, if extrapolated linearly in $1/N$, are consistent with conjugation lengths of polyacetylene of $\sim$40 double bonds. Similar values are suggested by parallel arguments involving the optical absorption frequencies of these molecules.[25]

This all assumes, of course, the validity of a linear extrapolation beyond $N = 12$. Numerous workers have assumed this validity, but it should be recognized that it has no *a priori* justification. Zerbi and co-workers[23] have shown that the Raman frequencies may be determined only following calculation of the phonon force fields, and that these force fields are a function of the conjugation length. Thus the dependence of a Raman frequency on conjugation may be only coincidentally linear over a given range; for this reason we considered it superfluous to fit the full range of the Raman shift vs inverse conjugation plots with forms more complicated than linear. Hence, at this point in time, it is prudent to await interpretation of our data in the framework of Zerbi *et al.* before commenting further on such an extrapolation.

In Fig. 5, we have plotted the Raman shifts vs band gap frequency for the polyenes and for polyacetylene. The polyacetylene data were obtained from the photoselection experiments of Ehrenfreund *et al.* Though the two data sets are in qualitative agreement, as we noted above, the Raman shifts for the polyenes appear systematically larger than for polyacetylene. That is, the Raman frequency obtained by excitation with a photon of given energy corresponds to that of a polyene having energy gap on the order of 0.4 eV (or approximately twice the $R\,4$ frequency) less than the excitation photon. In spite of this, we reiterate that the dependence of the Raman shift on band gap for the polyenes closely follows the dependence of the Raman shift vs laser frequency in polyacetylene, thereby *giving strong support for the standard model that the laser frequency is selecting conjugated chains of a specific conjugation length in the disordered polyacetylene films.*
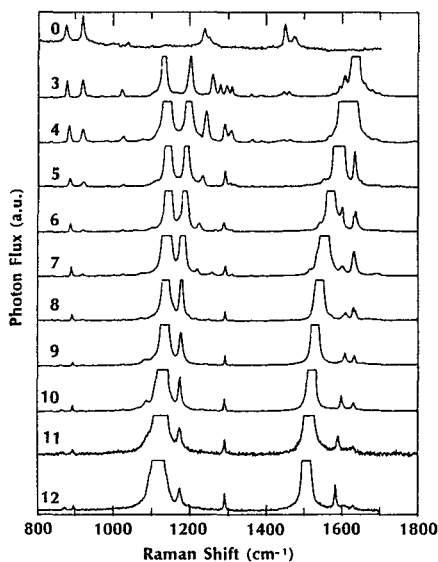

FIG. 7. Raman scattering spectrum of *t*-butyl capped polyenes, for 3–12 double bonds, as well as di(*t*-butyl). The vertical scale is an expansion of that of Fig. 2 by a factor of 30. Room temperature spectra were corrected for response of collecting optics/monochromator/detector. N is the number of double bonds.

In fact, Fig. 5 is remarkably similar to a plot in Ref. 39, in which, in place of our polyene shifts as a function of optical absorption peak, are plotted Raman shifts as a function of the peak of their respective sliced excitation profile in highly oriented polyacetylene. The comparison of Ref. 39 might be ascribed to a convolution of natural phonon widths with higher scattering amplitude for lower shift, but the results here suggest that whatever chemical defects limit the effective conjugation length in polyacetylene samples affect differently the electronic excitation energies and the vibrational frequencies.

As we pointed out above, the relative intensities of the R 1 plus R 2 Raman lines to the R 4 Raman line increases with increasing number of conjugated double bonds. This observation is in good agreement with the data on polyacetylene assuming again that the laser selects chains of a given conjugation length in the polyacetylene film. This trend has been explained via theoretical models of the vibrational structure by Ehrenfreund et al.[6,13-16] and by Zerbi et al.[19-24] The latter authors use a more complete vibrational analysis for the molecule and, therefore, may be able to explain the rather complex Raman structure we find in the small polyenes. We note that such structure is also present in the Raman spectra of polyacetylene, but has been ignored up to now. For example, the effects of the t-butyl groups are marked in the short chain polyenes (see Fig. 4) where the nominal single bond region is quite complicated. These features decrease in intensity as the chains become longer, confirming their association to the chain ends. Similar structure can be seen in the shorter laser wavelength Raman spectra of polyacetylene, suggesting the presence of crosslinked (i.e., sp_3 carbon chain ends) segments in the polyacetylene films.

We now consider the results in the context of the AM model of Horovitz et al.,[6,13-16] which begins with the Hamiltonian for the vibrations of a conjugated chain

$$H = \sum_n \frac{1}{2} \{ p_n^2 + (\omega_n^0)^2 q_n^2 \} + E_\pi(Q), \tag{2}$$

where q_n is the nth bare normal coordinate (in the absence of π electrons), ω_n^0 is the frequency of that bare mode, and E_π is the potential energy due to the π electrons. The basic assumption is that E_π is independent of the momenta $\{p_n\}$ (adiabatic approximation) and depends on the $\{q_n\}$ only via the dimerization coordinate Q, which is a linear combination of normal modes:

$$Q = \sum_n (2\lambda_n)^{1/2} \omega_n^0 q_n. \tag{3}$$

Here λ_n is the electron–phonon coupling constant for mode n. By expanding Eq. (2) to quadratic terms in q_n, new equilibrium positions, normal modes and frequencies can be found with the standard approach. The equation for the frequencies is found to be

$$D_0(\omega) \equiv \sum_n \frac{\lambda_n}{\lambda} (\omega_n^0)^2 [\omega^2 - (\omega_n^0)^2]^{-1} = -(1 - 2\tilde\lambda)^{-1}, \tag{4}$$

where $\lambda = \Sigma \lambda_n$, and the phonon renormalization parameter $\tilde\lambda$ is given by

$$2\tilde\lambda = 1 - 2\lambda E_\pi''(Q_{\rm eq}). \tag{5}$$

Note that in Eq. (4), both the second derivative of the π energy evaluated at the new equilibrium position $E_\pi''(Q_{\rm eq})$ and the total electron–phonon coupling λ determine $\tilde\lambda$, and both E_π'' and $\tilde\lambda$ are implicit functions of the conjugation length.

The roots of Eq. (4) are the new Raman frequencies ω_n^R as a function of $\tilde\lambda$. Note that as a particular λ_n decreases, the nth root of Eq. (4) increases toward ω_n^0. Hence, within this model, the increase in the R 0 frequencies with conjugation length may be due to a decrease in coupling of this mode native to the capping groups as the size of the molecule increases. From Eq. (4), a product rule[13] can be derived (by examining the algebraic equation in ω^2)

$$\prod_n \left[\frac{\omega_n^R}{\omega_n^0} \right]^2 = 2\tilde\lambda. \tag{6}$$

Within the Peierls model $\tilde\lambda = \lambda$,[15,40] and the energy gap is due entirely to bond alternation

$$E_g = 4E_c \exp\left(\frac{-1}{2\lambda} \right), \tag{7}$$

where E_c is an electron cutoff energy.[40]

Ehrenfreund et al. have tested this relationship by plotting $\prod_n (\omega_n^*/\omega_n)^2$ vs ln (E_g) in which the * denotes the frequency for one particular photon energy, for the case of three coupled modes.[6,16] They have found a nearly linear relationship of the form

$$\frac{2\tilde\lambda^*}{2\tilde\lambda} = \prod_n \left[\frac{\omega_n^*}{\omega_n} \right]^2 = A - B \ln(E_g), \tag{8}$$

in which $A = 3.23$ and $B = 0.44/2\tilde\lambda$ (for E_g measured in eV), as would be expected for the Peierls model.

In their fitting procedure, Ehrenfreund et al. have assumed that the bare frequencies $\{\omega_n^0\}$ do not change with E_g. They are then able to deduce a set of three bare frequencies, which in our notation are $\omega_1^0 = 1230$ cm^{-1}, $\omega_3^0 = 1310$ cm^{-1}, and $\omega_4^0 = 2040$ cm^{-1}, from the Raman frequencies for a series of excitation energies.[14,16] They did not use the intensity information in their fitting procedure.

In Fig. 8 we have followed the procedure of Ehrenfreund et al. in plotting $\prod_n (\omega_n^*/\omega_n)^2$ vs ln E_g, with E_g in eV for the polyenes $N = 6$ to 12, and compared the results to those for polyacetylene. The shorter polyenes have been omitted for two reasons: (1) we do not have solid state optical absorption data for them, and (2) for the shortest ones, finite length effects have split the modes, preventing direct comparison with the longer molecules. Whereas Ehrenfreund et al. enter three modes into their calculation, we have entered the five obviously coupled modes R 0→R 4. Ehrenfreund et al. have used the measured shifts at 2.60 eV photon energy for their reference frequencies ω_n^*, and we have likewise used the measured shifts for the 8-ene, for which $E_g = 2.60$ eV, for our reference frequencies. It should be noted in light of Fig. 5, that the comparison is not necessarily direct, in that Ehrenfreund et al. are probing chain segments having lower shift frequencies. The figure shows that the two sets of data are fit by straight lines having nearly
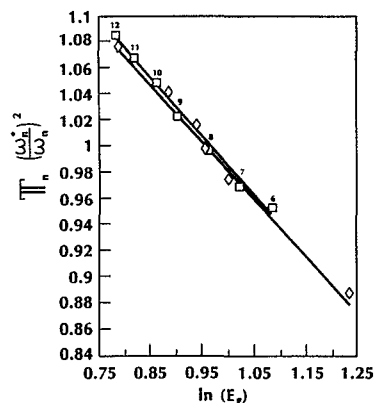
FIG. 8. Dependence (squares) of the product $\Pi_n (\omega_n^*/\omega_n)^2$ on $\ln(E_g)$ with E_g in eV. For comparison, we show (diamonds) data of Ehrenfreund et al., (Ref. 16) in which case E_g is the excitation photon energy. In both cases the products are normalized to their values at 2.60 eV, and the lines are the best fit to the respective data set.

TABLE II. Results of AM model fit to Raman frequencies for $N = 7$–12 including four modes (R 1 to R 4) and comparison to three-mode results of Ehrenfreund et al. (Ref. 16).

Mode	This work		Reference 16	
	ω_n^0	λ_n	ω_n^0	λ_n
1	1160	0.01	$\cdots$	$\cdots$
2	1230	0.11	1230	0.07
3	1300	0.04	1310	0.02
4	1820	0.84	2040	0.91

identical slopes (our fit: $B = 0.45/2\tilde{\lambda}$ *). (If we include only four modes, R 1→R 4, B increases by roughly 10%.) Thus the simplest application of the amplitude mode model to our data, with consideration of the two additional modes, suggests that the product $(2\tilde{\lambda}) = \Pi_n (\omega_n/\omega_n^0)^2$ in the small polyenes is related directly to the conjugation length. However, this dependence of $\Pi\omega_n$ vs $\ln E_g$ can arise in ways different from the Peierls relationship (7), as outlined in the Appendix.

We have followed the procedure of Ehrenfreund et al. in attempting to determine a conjugation-length independent set of bare frequencies and coupling constants. As noted above, the coupling constant for the R 0 mode is not independent of conjugation length. However, the coupling for this mode is relatively weak, so we have fit the Raman frequencies of R 1–R 4 exclusively. The parameters so determined, listed in Table II, provide a good fit (± 2 cm^{-1}) to the Raman shifts (i.e., the fit is self-consistent). The bare frequency ω_4^0 is approximately 200 cm^{-1} lower than the value determined by Ehrenfreund et al.[16] As we note below in discussing the single-molecule fits, the value of the highest bare frequency is the most sensitive to variations in the experimental data. More important, however, is the necessity of having λ_3 thrice greater than λ_1 in order to fit the data, which given the relative intensity and frequency behaviors of these two modes, together with the previously determined value of λ_3 and the interpretation of Zerbi et al. of the dynamics of this particular mode, we find highly unphysical. This can only suggest that the product rule (6) is more general than the Hamiltonian (2) and its solution (4).

The amplitude mode model also provides an expression for the cross section for Raman scattering,[14–16] and in particular it can be shown that the intensities of the peaks are proportional to the residues of the conductivity at the peak positions (which are themselves given by the poles of the conductivity), i.e.,

$$I_n^R \sim [D_0'(\omega_n^R)]^{-1}. \tag{9}$$

Thus from measurement of the Raman shifts $\{\omega_n^R\}$ and rela-

tive intensities $\{(I_n^R/I_{ref}^R)\}$ for a single member of the series, it is in principle possible to determine N-specific (i.e., not conjugation independent) bare frequencies $\{\omega_n^0\}$ and relative coupling constants $\{\lambda_n/\lambda\}$ that parametrize the phonon propagator $D_0(\omega)$. We have attempted to determine most likely bare frequencies and coupling constants, with uncertain results. Since for N peaks we have $2N - 1$ unknowns [N bare frequencies but only $N - 1$ coupling constants, because $\Sigma(\lambda_n/\lambda) = 1$] but only $2N$-2 equations [N–1 equations relating relative intensities of N peaks, via ratios of Eq. (9), and $N - 1$ equations of form $D_0(\omega_i^R) = D_0(\omega_{i+i}^R)$], this procedure required arbitrarily fixing one of the parameters to be determined. We fixed the third bare frequency at 1310 cm^{-1}, the value determined by Ehrenfreund et al., because the frequency and intensity of this mode vary little through the polyene series, as in polyacetylene. While there were no recognizable trends in the bare frequencies as a function of N, we did notice that the highest bare frequency, which was the one consistently found to be the one most strongly coupled (as in polyacetylene), was the most sensitive to the qualitative fit. In general, we were unable to determine sets of parameters that accurately reproduced all of the observed oscillator strengths; this is consistent with the statement of Ehrenfreund et al. that the intensity of the mode at 1292 cm^{-1} is not accurately given by the AM model.[16] Nor do the intensities given by Eq. (9), using the conjugation-independent parameters of Table I, provide a good fit to the intensity data. This is not surprising since the intensities depend upon the detailed expression for the cross section in the AM model, which is a rather sensitive function of the parameters of that model. In addition, it should be noted that the cross section calculated by Horovitz does not consider higher order vibrational coupling nor σ-electron polarizability, both of which may be important, so that one might reasonably expect the theory to accurately predict the oscillator strengths of only the most strongly coupled modes. The failure of the AM model to predict intensity of the R 1 and R 4 modes implies questionable validity to their fits to polyacetylene data for R 1 and R 4.

The AM model assumes the existence of three bare modes with eigenvectors and frequencies independent of $\tilde{\lambda}$, i.e., of conjugation length. Diagonalization of the Hamiltonian (2), in which the $\{q_n\}$ enter into the added potential E_π [via Eq. (3)], necessarily provides a new set of normal modes with frequencies given by the roots of Eq. (4). Presumably, one could calculate for these new (actual) modes a set of effective electron–phonon coupling constants, which

would directly give the relative Raman intensities. However, without a detailed expression for $E_\pi(Q)$ the normal modes are not obtainable. Thus the Raman shifts and the oscillator strengths are always expressed, in this model, in terms of the bare modes and their respective electron–phonon coupling constants, together with a varied value of $\tilde{\lambda}$. Clearly, the assumption of fixed bare modes is not valid for the shortest of conjugation lengths, in which we observe mode splitting. However, conjugation lengths this short are presumably only in the tail of the length distribution of *trans*-polyacetylene.

In contrast to the formal model (2), Zerbi and co-workers have offered a microscopic model of vibrational modes in polyenes.[19–23] This begins with the observation that the product rule (6) is similar to the produce of eigenvalues of modes obtained from the familiar FG matrix formalism. One can imagine a set of (five) in-plane molecular coordinates for the polyene chain, which are not normal modes, one of which represents an out-of-phase (of C = C with respect to C–C) carbon–carbon stretch mode.[19] Only the force constant for this particular coordinate depends upon the conjugation length, i.e., on the stiffness of the π electrons. Diagonalization of the resulting dynamical matrices having off-diagonal elements coupling the various modes results in a set of normal modes whose eigenvectors and frequencies explicitly depend upon the force constant for the out-of-phase stretch, i.e., on the conjugation length. The varied oscillator strength ratio (I_{R1}/I_{R2}) is then explained in terms of the relative projections of the normal modes onto the dimerization amplitude coordinate Q, which is the only one that should be strongly coupled to the excited states.

The trend of the data in Fig. 6 is in the same direction as that predicted by the Milan group.[20,23] Furthermore, their work allows correlation of the ratios with specific values of the force constant for the out-of-phase stretch, on the order of 3–5 mdyn/Å (decreasing with conjugation). This range is in comparison to the value of 6.14 mdyn/Å for the C = C stretch in butadiene.[41,42] That is, the extent of conjugation has reduced the π-electron stiffness by a factor of about 2 for the longest molecules. In sum, the data of Fig. 6 confirm the conjugation length dependence of the normal modes, and together with the frequency data should allow calculation of the dependence of the π-electron energy on the dimerization amplitude, or the conjugation length.

One could, if one wished, identify three of Zerbi's molecular coordinates with the three bare modes of the AM model. There are, however, two difficulties with this. (1) The bare modes of the AM model must be the normal modes of the polyene in the absence of π-electron coupling, whereas the molecular coordinate of the Zerbi model may not be normal modes. (2) Zerbi and co-workers have considered only one other molecular coordinate (CH wagging) to be coupled to the dimerization amplitude, and thus would need only two electron–phonon coupling constants to explain the data. On the other hand, the success of the product rule (6), which was derived on the assumption of bare modes independent of conjugation, as evidenced by Fig. 8 and Table I, may be considered as support for that assumption. (See, however, the Appendix.) At this time, then we cannot reach any definite

conclusions concerning the relevance of the bare modes of the AM model, and these questions should be enlightened by future calculations.

We return, finally, to the question of alternative models for the scattering spectra of *trans*-polyacetylene discussed in Sec. I. Because of the powder or microcrystalline form of the samples, we were unable to obtain reliable excitation profiles for the Raman scattering, which would certainly have tested the validity of either model. Nevertheless, at this time it would be most interesting to learn if incorporation of the results presented in this paper into the Brivio–Mulazzi model allows that model to explain the Raman dispersion by a unimodal distribution of conjugation lengths. Such a result would provide a satisfying convergence of the two approaches to calculating the Raman cross section.

V. CONCLUSIONS

In this paper, we have measured the Raman spectra of short polyenes as a function of conjugation length, and attempted to interpret the results within the framework of the standard models. We find

(i) The AM model, using conjugation length independent parameters, provides a reasonable representation of the chain length dependence of the measured Raman frequencies for our model polyenes. However, the parameters needed to fit the data are found to be unphysical. Furthermore, it is unable to predict the intensities of the coupled models. This weakness is consistent with previous findings.[16] Use of the intensity data to provide N-specific bare parameters was also unsuccessful.

(ii) The variation of the Raman spectra with conjugation length resembles that of the variation of the Raman spectra of polyacetylene with laser frequency. We suggest, therefore, that this is evidence for the idea that conjugation length is the controlling parameter for both the polyene and polyacetylene data, although Fig. 5, together with the similar result in Ref. 39, caution against direct extrapolation of vibrational frequencies from polyenes to polyacetylene. (Note that this correlation can be accommodated within the AM model since both E''_π and $\tilde{\lambda}$ are implicit functions of conjugation length.) In particular, this deduction calls into question the statement[43] that the slope of the $\tilde{\lambda}$ plot (Fig. 8) in polyacetylene serves as evidence for the validity of an electron–phonon (pure Peierls) coupling model of polyacetylene. As shown in the Appendix, an inverse conjugation dependence in the band gap and the Raman frequencies provides this same $\tilde{\lambda}$ plot.

(iii) The recent molecular dynamics calculations of Zerbi and co-workers provide a starting point for an analytical understanding of A_g vibrations in polyenes. When applied to the data presented here, their approach suggests that polyene normal modes are a function of the coherence length of the charge density wave to which they are coupled.

ACKNOWLEDGMENTS

APPENDIX

There seems to be a contradiction between the experimentally determined dependence of E_g and ω_n on $1/N$, the number of double bonds or conjugation length (as exemplified in Figs. 3 and 4) and the logarithmic dependence used in the above analysis. However, our data can be manipulated into this form by writing

$$E_g = A + B/N \tag{A1}$$

$$\omega_n = a_n + b_n/N. \tag{A2}$$

Therefore,

$$\prod_n \left[\frac{\omega_n^*}{\omega_n} \right]^2 \equiv \prod_n \frac{[1 + (b_n/a_n)(1/N^*)]^2}{[1 + (b_n/a_n)(1/N)]^2}$$

$$\cong 1 + 2\sum_n \frac{b_n}{a_n} (N^{*-1} - N^{-1}) \tag{A3}$$

and

$$\frac{E_g}{E_g^*} = 1 + \frac{B}{A}(N^{-1} - N^{*-1}) + \cdots$$

$$= \exp \frac{B}{A}(N^{-1} - N^{*-1}) \tag{A4}$$

or

$$(N^{-1} - N^{*-1}) = (A/B)\ln\left(\frac{E_g}{E_g^*}\right), \tag{A5}$$

so that

$$\prod_n \left[\frac{\omega_n^*}{\omega_n} \right]^2 \cong 1 - 2\sum_n \frac{b_n}{a_n} \frac{A}{B} \ln(E_g/E_g^*), \tag{A6}$$

which is the desired relationship.

[1] I. Harada, Y. Furukawa, M. Tasumi, H. Shirakawa, and S. Ikeda, J. Chem. Phys. **73**, 4746 (1980).

[2] L. S. Lichtmann, A. Sarhangi, and D. B. Fitchen, Solid State Commun. **36**, 869 (1980).

[3] H. Kuzmany, Phys. Status Solidi B **97**, 521 (1980).

[4] S. Lefrant, J. Phys. (Paris) Colloq. **44**, C3-C247 (1983).

[5] E. Mulazzi, G. P. Brivio, E. Faulques, and S. Lefrant, Solid State Commun. **46**, 851 (1983).

[6] Z. Vardeny, E. Ehrenfreund, O. Brafman, and B. Horovitz. Phys. Rev. Lett. **51**, 2326 (1983).

[7] G. P. Brivio and E. Mulazzi, Chem. Phys. Lett. **95**, 555 (1983).

[8] G. P. Brivio and E. Mulazzi, Phys. Rev. B **30**, 876 (1984).

[9] (a) L. Rimai, M. E. Heide, and D. Gill, J. Amer. Chem. Soc. **95**, 4493 (1973); (b) T. M. Ivanova, L. A. Yanovskaya, and P. P. Shorygin, Opt. Spectrosc. **18**, 115 (1965); (c) Y. Furukawa, T. Arakawa, H. Takeuchi, I. Harada, and H. Shirakawa, J. Chem. Phys. **81**, 2907 (1984).

[10] L. S. Lichtmann, Ph. D. thesis, Cornell University, 1981.

[11] E. Mulazzi, R. Tubino, and G. Dellepiane, Chem. Phys. Lett. **86**, 347 (1982).

[12] M. A. Schen, J. C. W. Chien, E. Perrin, S. Lefrant, and E. Mulazzi, J. Chem. Phys. **89**, 7615 (1988).

[13] B. Horovitz, Solid State Commun. **41**, 729 (1982).

[14] B. Horovitz, Z. Vardeny, E. Ehrenfreund, and O. Brafman, Synth. Met. **9**, 215 (1984).

[15] B. Horovitz, Z. Vardeny, E. Ehrenfreund, and O. Brafman, J. Phys. C **19**, 7291 (1986).

[16] E. Ehrenfreund, Z. Vardeny, O. Brafman, and B. Horovitz, Phys. Rev. B **36**, 1535 (1987).

[17] R. Tiziano, G. P. Brivio, and E. Mulazzi, Phys. Rev. B **31**, 4015 (1985); E. Mulazzi and G. P. Brivio, Mol. Cryst. Liq. Cryst. **105**, 233 (1984).

[18] K. Knoll and R. R. Schrock, J. Amer. Chem. Soc. **111**, 7989 (1989).

[19] C. Castiglioni, J. T. Lopez Navarrete, G. Zerbi, and M. Gussoni, Solid State Commun. **65**, 625 (1988).

[20] G. Zerbi, C. Castiglioni, J. T. Lopez Navarrete, T. Bogang, and M. Gussoni, Synth. Met. **28**, D359 (1989).

[21] M. Gussoni, C. Castiglioni, and G. Zerbi, Synth. Met. **28**, D375 (1989).

[22] J. T. Lopez Navarette and G. Zerbi, Synth. Met. **32**, 151 (1989).

[23] G. Zerbi, C. Castiglioni, B. Tian, and M. Gussoni, in *Electronic Properties of Conjugated Polymers III*, edited by H. Kuzmany, M. Mehring, and S. Roth, Springer Series in Solid State Sciences, Vol 91 (Springer, New York, 1989), p. 106.

[24] G. Zerbi, in *Applied Fourier Transform Infrared Spectroscopy*, edited by M. Mackenzie (Wiley, New York, 1988).

[25] H. E. Schaffer, R. R. Chance, K. Knoll, R. R. Schrock, and R. Silbey, in *Conjugated Polymeric Materials: Opportunities in Electronics, Optoelectronics, and Molecular Electronics*, edited by J. L. Bredas and R. R. Chance (Kluwer Academic, Dordrecht, 1990), p. 365.

[26] D. G. Cameron, J. K. Kauppinen, D. J. Moffat, and H. H. Mantsch, Appl. Spectros. **36**, 245 (1982).

[27] F. F. Cleveland, J. E. Lamport, and R. W. Mitchell, J. Chem. Phys. **18**, 1320 (1950).

[28] J. L. Bredas, R. Silbey, D. Boudreaux, and R. Chance, J. Amer. Chem. Soc. **105**, 6555 (1983).

[29] L. Salem, *The Molecular Orbital Theory of Conjugated Systems* (Benjamin, Reading, 1966), and references therein.

[30] L. A. Sklar, B. Hudson, M. Peterson, and J. Diamond, Biochemistry **16**, 813 (1977).

[31] B. Kohler, J. Chem. Phys. **93**, 5838 (1990).

[32] F. Zerbetto, M. Z. Zgierski, and G. Orlandi, Chem. Phys. Lett. **141**, 138 (1987).

[33] M. L. Shand, R. R. Chance, M. LePostollec, and M. Schott, Phys. Rev. B **25**, 4431 (1982).

[34] H. Eckhardt and co-workers (unpublished).

[35] F. W. Langkilde, R. Wilbrandt, O. F. Nielsen, D. H. Christensen, and F. M. Nicolaisen, Spectrochim. Acta *A* **43**, 1209 (1987).

[36] A. B. Myers and K. S. Pranata, J. Phys. Chem. **93**, 5079 (1989), and references therein.

[37] H. E. Schaffer, R. H. Friend, and A. J. Heeger, Phys. Rev. B **36**, 7537 (1987).

[38] Z. Vardeny, E. Ehrenfreund, O. Brafman, B. Horovitz, H. Fujimoto, J. Tanaka, and M. Tanaka, Phys. Rev. Lett. **57**, 2995 (1986).

[39] P. Knoll, H. Kuzmany, and G. Leising, in *Electronic Properties of Conjugated Polymers*, edited by H. Kuzmany, M. Mehring, and S. Roth, Springer Series in Solid State Sciences, Vol. 76 (Springer, Berlin, 1987), p. 134.

[40] B. Horovitz and J. A. Krumhansl, Solid State Commun. **26**, 81 (1978).

[41] P. Pulay, G. Fogarisi, G. Pongor, J. E. Boggs, A. Vargha, J. Amer. Chem. Soc. **105**, 7037 (1983).

[42] H. Yoshida and M. Tasumi, J. Chem. Phys. **89**, 2803 (1988).

[43] Z. Vardeny, E. Ehrenfreund, O. Brafman, and B. Horovitz, Phys. Rev. Lett. **54**, 75 (1985).